THE JOURNAL OF BIOLOGICAL CHEMISTRY VOL. 289, NO. 33, pp. 23200–23208, August 15, 2014

NADPH Oxidase 4 Induces Cardiac Arrhythmic Phenotype in Zebrafish*[S]

Received for publication, June 6, 2014 Published, JBC Papers in Press, June 24, 2014, DOI 10.1074/jbc.M114.587196

Yixuan Zhang[‡], Hirohito Shimizu[§], Kin Lung Siu[‡], Aman Mahajan[‡], Jau-Nian Chen[§], and Hua Cai[‡1]

From the [‡]Divisions of Molecular Medicine and Cardiology, Departments of Anesthesiology and Medicine, Cardiovascular Research Laboratories, David Geffen School of Medicine at UCLA and the [§]Department of Molecular, Cell and Developmental Biology, UCLA, Los Angeles, California 90095

Background: Oxidative stress has been implicated in arrhythmia without a defined causal relationship.
Results: Overexpression of NOX4 in zebrafish embryos induces arrhythmic phenotype via ROS and CaMKII.
Conclusion: NADPH-driven ROS production and subsequent CaMKII activation mediate NOX4-dependent arrhythmogenesis.
Significance: Our data present the first evidence for a direct causal role of NOX4 in cardiac arrhythmia.

Oxidative stress has been implicated in cardiac arrhythmia, although a causal relationship remains undefined. We have recently demonstrated a marked up-regulation of NADPH oxidase isoform 4 (NOX4) in patients with atrial fibrillation, which is accompanied by overproduction of reactive oxygen species (ROS). In this study, we investigated the impact on the cardiac phenotype of NOX4 overexpression in zebrafish. One-cell stage embryos were injected with NOX4 RNA prior to video recording of a GFP-labeled (*myl7*:*GFP* zebrafish line) beating heart in real time at 24–31 h post-fertilization. Intriguingly, NOX4 embryos developed cardiac arrhythmia that is characterized by irregular heartbeats. When quantitatively analyzed by an established LQ-1 program, the NOX4 embryos displayed much more variable beat-to-beat intervals (mean S.D. of beat-to-beat intervals was 0.027 s/beat in control embryos *versus* 0.038 s/beat in NOX4 embryos). Both the phenotype and the increased ROS in NOX4 embryos were attenuated by NOX4 morpholino co-injection, treatments of the embryos with polyethylene glycol-conjugated superoxide dismutase, or NOX4 inhibitors fulvene-5, 6-dimethylaminofulvene, and proton sponge blue. Injection of NOX4-P437H mutant RNA had no effect on the cardiac phenotype or ROS production. In addition, phosphorylation of calcium/calmodulin-dependent protein kinase II was increased in NOX4 embryos but diminished by polyethylene glycol-conjugated superoxide dismutase, whereas its inhibitor KN93 or AIP abolished the arrhythmic phenotype. Taken together, our data for the first time uncover a novel pathway that underlies the development of cardiac arrhythmia, namely NOX4 activation, subsequent NOX4-specific NADPH-driven ROS production, and redox-sensitive CaMKII activation. These findings may ultimately lead to novel therapeutics targeting cardiac arrhythmia.

Increased production of reactive oxygen species (ROS)[2] has been implicated in cardiovascular disorders, including hypertension, atherosclerosis, diabetic vascular complications, heart failure, and cardiac arrhythmia. Nonetheless, unlike an established causal role of oxidative stress in vascular pathogenesis, it remains unclear whether oxidative stress contributes to the initiation of arrhythmic disorders in the heart. Accumulating evidence has implicated an emerging role of NADPH oxidase (NOX) in atrial fibrillation (AF), although a causal relationship has never been evaluated (1–4). Our recent study has demonstrated a marked up-regulation of the specific NADPH oxidase isoform 4 (NOX4) in patients with AF, which is accompanied by overproduction of reactive oxygen species, especially in patients with hypertension, a known risk factor for AF (5). Therefore, in this study we aimed to investigate whether overexpression of NOX4 in zebrafish directly induces cardiac arrhythmic phenotype.

Zebrafish is a valuable model for studies of cardiovascular physiology (6). One of the advantages of zebrafish is that during early development, the heart is situated prominently at the ventral side of the embryo, wrapped by a thin pericardial membrane, and is transparent. Using a cardiac-specific green fluorescent protein (GFP) transgenic fish line, it is convenient to monitor cardiac development and function in real time, by video taping the beating heart noninvasively. In addition, genetic manipulations can be rapidly achieved by morpholino (MO) or RNA injection. Hence, we can perform both gain-of-function and loss-of-function studies of the target gene in a relatively short period of time. Another advantage of the zebrafish model is that the heart rate of zebrafish is not very

* This work was supported, in whole or in part, by National Institutes of Health Grants HL077440 and HL088975 (to H. C.), HL108701 (to H. C. and D. G. H.), HL119968 (to H. C.), and HL096980 (to J. N. C.) from NHLBI. This work was also supported by American Heart Association Established Investigator Award 12EIA8990025 (to H. C.).

[S] This article contains supplemental Videos I and II.

[1] To whom correspondence should be addressed: Divisions of Molecular Medicine and Cardiology, Dept. of Anesthesiology and Medicine, Cardiovascular Research Laboratories, David Geffen School of Medicine at UCLA, 650 Charles E. Young Dr., Los Angeles, CA 90095. Tel.: 310-267-2303; Fax: 310-825-0132; E-mail: hcai@mednet.ucla.edu.

[2] The abbreviations used are: ROS, reactive oxygen species; NOX4, NADPH oxidase isoform 4; AF, atrial fibrillation; MO, morpholino; NOX, NADPH oxidase; hpf, hours post-fertilization; NOX4-P437H, catalytically inactive NOX4 mutant; PEG-SOD, polyethylene glycol-conjugated superoxide dismutase; CaMKII, calcium/calmodulin-dependent protein kinase II; DCFH-DA, 2′,7′-dichlorofluorescein diacetate; Ful-5, fulvene-5; 6-Ful, 6-dimethylamino-fulvene; hNOX4, human NOX; Tempo, 2,2,6,6-tetramethyl-L-piperidinyloxy; AIP, autocamtide-2-related inhibitory peptide II.

different from human heart rate. In contrast, the murine heart beats 7–10 times faster than the human heart, which makes it difficult to either induce or observe arrhythmia. Furthermore, even with severe cardiac dysfunctions that might be lethal to mice, zebrafish embryos most often survive for several days to enable phenotypical analyses (7). Previous studies have shown that zebrafish can be used as a good model system to identify and characterize cardiac arrhythmias resembling human diseases (7–9).

In this study, we used zebrafish as an *in vivo* model system to study the effects on heart rhythm of NOX4 overexpression. By transiently overexpressing wild type human NOX4 RNA in zebrafish, we found that NOX4-injected embryos developed an arrhythmic phenotype at 24–30 hours post-fertilization (hpf), which was characterized by irregular heartbeats that are qualitatively and quantitatively analyzed by video recordings and a custom-made LQ-1 program (9, 10). Co-injection with NOX4 ATG-morpholino abolished arrhythmic phenotypes and superoxide production. Injection of RNA encoding the catalytically inactive NOX4 mutant (NOX4-P437H) deficient in NADPH binding had no effect on cardiac phenotypes. Similar effects were also observed in polyethylene glycol-conjugated superoxide dismutase (PEG-SOD, cell-permeable superoxide scavenger) or NOX4 inhibitors treated NOX4-injected embryos (fulvene-5, 6-dimethylamino-fulvene, and proton sponge blue). NOX4-induced H_2O_2 production was inhibited by Tempo and fulvene-5. These data indicate that the arrhythmic phenotype is specifically induced by NOX4 and dependent on the ROS generating activity of NOX4. Interestingly, NOX4 overexpression resulted in increased calcium/calmodulin-dependent protein kinase II (CaMKII) phosphorylation at Thr-286. A selective inhibitor for CaMKII, autocamtide-2-related inhibitory peptide II (AIP), or KN93, also abolished the arrhythmic phenotype. In summary, our findings for the first time uncover a direct causal role of NOX4 in cardiac arrhythmia, which is mediated by the ROS producing activity of NOX4 and CaMKII activation.

EXPERIMENTAL PROCEDURES

Cloning and in Vitro RNA Transcription—Human NOX4 (NM_016931) full-length coding region was amplified from pCMV6-hNOX4 (OriGene, SC310253, Rockville, MD) by PCR and cloned into pCS2+ at ClaI and XhoI sites. NOX4-P437H was generated by PCR-based site-directed mutagenesis (KOD Hot Start, Novagen/EMD Millipore, Darmstadt, Germany). All of the plasmids were confirmed by sequencing. Capped mRNA of human NOX4 and mutant NOX4-P437H were synthesized by *in vitro* transcription with the mMESSAGE mMACHINE kit (Ambion).

Zebrafish Strains and Studies—Transgenic strain *myl7*:*GFP* zebrafish were maintained as described previously (7, 11). GFP expression is driven by a cardiac-specific promoter of *myl7* (also known as cardiac myosin light chain 2). The developmental stages of fish were determined by observations of morphological features of fish raised at 28.5 °C.

Micro-injection—Wild type human NOX4 or mutant NOX4-P437H RNA (300 pg) was injected into *myl7*:*GFP* transgenic embryos at one-cell stage. In some experiments, embryos were co-injected with 3 ng of antisense morpholino (5′-GCC-AGCTCCTCCAGGACACAGCCAT-3′, Gene Tools, Philomath, OR) complementary to the translation start codon ATG of the human NOX4 coding region.

Pharmacological Interventions—PEG-SOD (25 units/ml, Sigma), Tempo (10 μM, Sigma), autocamtide-2-related inhibitory peptide II (AIP, 1 μM, Calbiochem, EMD Millipore), 6-dimethylamino-fulvene (10 μM, Santa Cruz Biotechnology), and proton sponge blue (5 μM) or fulvene-5 (10 μM, last two as generous gifts from Dr. Jack Arbiser, Emory University, Atlanta, GA) were added to the E3 media soaking the embryos (5 mM NaCl, 0.17 mM KCl, 0.33 mM $CaCl_2$, 0.33 mM $MgSO_4$) at 23.5 hpf.

Video Analyses—Digital videos were taken under UV illumination from embryos of similar developmental stages at 24–30 hpf. Embryos were randomly chosen for videotaping. Each embryo was videotaped for 1 min, after stabilizing for 1–2 min in 0.01% Tricaine methanesulfonate (Sigma). The videos were split into consecutive frames by QuickTime player at 30 frames/s, which were then converted to a line-scanning result of atrial contraction by a custom-made LQ-1 program as described previously (Fig. 1, *A* and *B*) (9, 10). Each vertical line by LQ-1 analysis represents one contraction. The horizontal axis indicates time of contraction, 1/30 s/pixel. By measuring the number of pixels between every vertical line (contraction) by another custom-made software, we acquired the precise time for one contraction, considered as beat-to-beat interval (beat-to-beat interval = number of pixels × 1/30 s). To represent the beat-to-beat variation, we calculated standard deviation (S.D.) of beat-to-beat intervals of one embryo (Fig. 1, *E* and *F*). Statistical comparison was carried out between standard deviations of control and NOX4 or NOX4-P437H RNA-injected embryos. All the video analyses were done blindly without knowing the genotypes.

ROS Measurements—More than 20 embryos were harvested and homogenized in cold 1× lysis buffer (20 mmol/liter Tris-HCl, pH 7.4, 150 mmol/liter NaCl, 1 mmol/liter EDTA, 1 mmol/liter EGTA, 2.5 mmol/liter sodium pyrophosphate, 1 mmol/liter β-glycerophosphate, 1 mmol/liter sodium orthovanadate, 1% Triton X-100, supplemented with protease inhibitor mixture) at 27–33 hpf. On average, 5 μl of lysis buffer was used per embryo. The samples were centrifuged at 12,000 rpm at 4 °C for 15 min after sitting on ice for 10–15 min, and then the supernatant was transferred to a new 1.7-ml Eppendorf tube for superoxide determination using electron spin resonance (ESR) (eScan, Bruker) immediately (12–17). For each measurement, 5 μl of protein lysate was loaded. The rate of superoxide production was presented as micromolar/min/mg of protein after normalizing ESR data to protein. For *in vivo* H_2O_2 detection, embryos (30 hpf) were incubated with 2′,7′-dichlorofluorescein diacetate (DCFH-DA, Sigma, 20 μM) in the dark for 1 h at 28.5 °C and washed three times as described previously (18). Embryos were randomly transferred to 0.01% Tricaine methanesulfonate buffer for imaging. All fluorescence images were taken at the same setting by Carl Zeiss Stemi SV 11 Apo microscope with 488 nm wavelength excitation. The average fluorescence density (normalized to area) was analyzed by ImageJ.

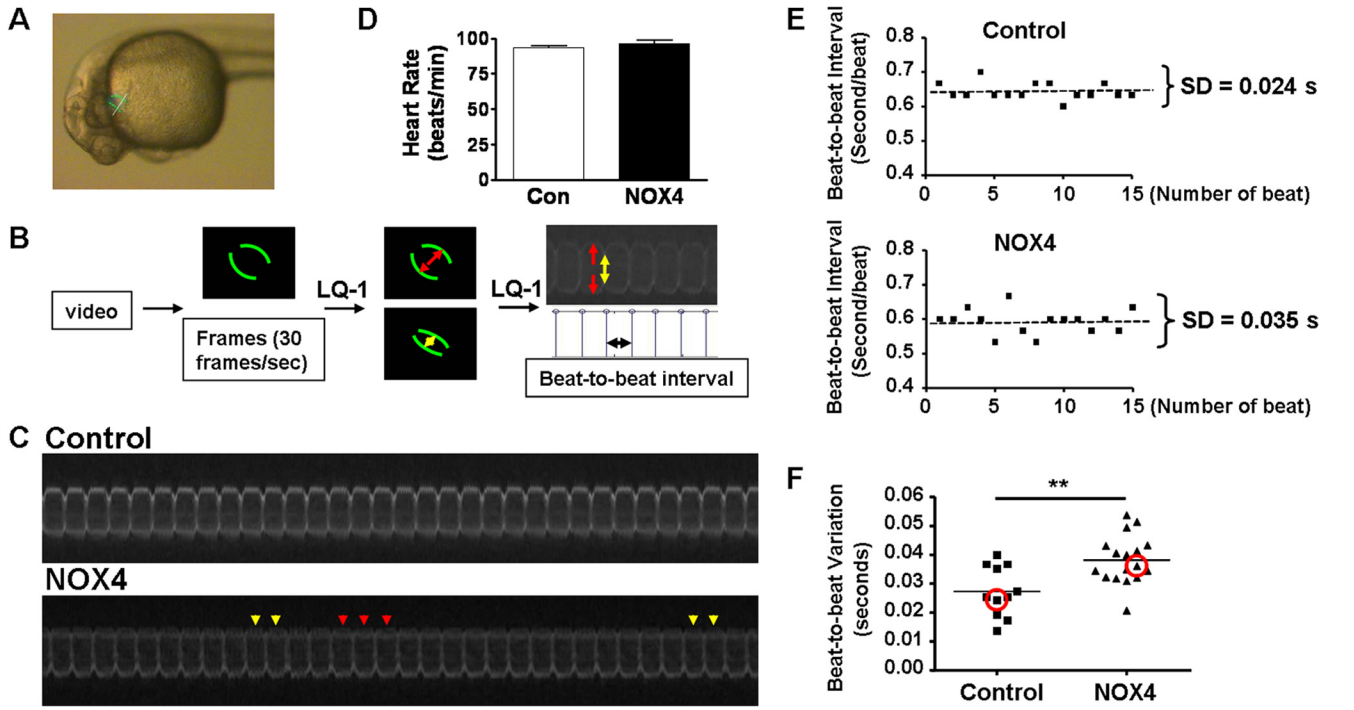

FIGURE 1. **NOX4 overexpression induces cardiac arrhythmia in zebrafish embryos, quantitative analyses.** *A,* representative *myl7*:*GFP* zebrafish embryo. The outline of the heart is marked in *green*. *White line* indicates scanning line position of the LQ-1 program. *B,* flow chart demonstrating video analyses and measurements of beat-to-beat intervals. *Red* and *yellow arrows* indicate heart relaxation and contraction, respectively. *Black arrow* indicates a beat-to-beat interval. *C,* representative LQ-1 plots of beat-to-beat intervals against time to demonstrate beat-to-beat variations. Note the faster beats (*yellow arrowheads*) and the slower heartbeats (*red arrowheads*) in NOX4 RNA-injected embryos. *D,* heart rates in control and NOX4 embryos at 24–30 hpf. $n = 11$ and 17. *E, dotted lines* mark average beat-to-beat intervals of representative embryos, and the standard deviations are calculated. *F,* distributions of beat-to-beat variations of control and NOX4 RNA-injected embryos. *One dot* represents standard deviation of one embryo. *Red circles* indicate standard deviations in *E*. **, $p < 0.01$ *versus* control. $n = 11$ and 17.

Immunoblot Analysis—Tissue lysates of zebrafish embryos were prepared as mentioned above. Phosphatase inhibitor mixtures 2 and 3 (1:100, Sigma) were added when necessary. For determination of CaMKII (Thr-286) phosphorylation, 200 μg of proteins were separated in 10% SDS-PAGE with detection using 1:500 primary antibody dilution (Cell Signaling Technology). Densitometry was performed with ImageJ and normalized to tubulin.

Whole Mount Staining of Zebrafish Embryos and Confocal Microscopy—Whole mount antibody staining was performed as described previously (19). Briefly, embryos were fixed in 4% paraformaldehyde in phosphate-buffered saline (PBS), followed by acetone penetration. Embryos were blocked in 2% BSA + 5% donkey serum in PBST (PBS + 0.1% Triton X-100) and stained with anti-phospho-CaMKII (Thr-286) (1:100, Cell Signaling Technology) and donkey anti-rabbit 555 (1:100, Invitrogen) overnight at 4 °C. Hearts were dissected out and embedded in 1% low melting agarose (Sigma) before imaging. Confocal Z-stack images were taken by Nikon Eclipse Ti microscope using ×20 objective.

Statistical Analysis—All the data are shown as means ± S.E. Data were analyzed by Student's *t* test or analysis of variance followed by a Newman-Keuls post hoc analysis. Statistical significance is set as $p < 0.05$. For phenotype incidence comparisons shown in Table 1, data were analyzed between the NOX4 injection- and inhibitor-treated groups using 2-by-2 contingency tables and the χ^2 coupled with the Fisher exact test (two-tailed). *p* value of each comparison is shown in Table 1. Treatments were considered different if $p < 0.05$.

RESULTS

Overexpression of NOX4-induced Cardiac Arrhythmic Phenotype in Zebrafish—Based on the fact that oxidative stress has been implicated in the pathogenesis of atrial fibrillation despite an unclear causal relationship (1, 2, 4, 5, 20–22), and our recent findings that NOX4 is markedly up-regulated in human patients with AF (5), we overexpressed human (h) NOX4 RNA in zebrafish embryos to study its functional consequences in modulating cardiac phenotypes *in vivo*. By injecting 300 pg of wild type hNOX4 RNA into one-cell stage *myl7*:*GFP* transgenic embryos, we discovered that 53% of these embryos developed a phenotype of irregular heart beats at 24–30 hpf (supplemental Video I, representative videos from control or NOX4 RNA-injected embryos), although only 10% of control embryos had a phenotype of much less variable heart beats at the same developmental stage (19 out of 167), which is considered physiological (23, 24). Table 1 also summarized all phenotypic responses to molecular and pharmacological interventions described below. The arrhythmic phenotype is obvious up to 48 hpf, after which it is not easily visible any more, which is likely attributed to RNA degradation (Fig. 7*A*). Of note, efficacies of NOX4 overexpression and morpholino treatment (see below) were verified by transfecting a Myc-tagged NOX4 RNA and detecting NOX4 using the Myc antibody (supplemental Fig. II).

TABLE 1
Arrhythmic phenotype in NOX4 RNA-injected embryos with or without corresponding treatments
Data are combined from three or more independent injections.

Group	No. with phenotype	No. without phenotype	Total no. analyzed	Phenotype percentage	*p* value (*vs.* NOX4)
				%	
NOX4	133	118	251	53.0	
NOX4 + MO	12	47	59	20.3	$p < 0.001$
NOX4 + PEG-SOD	4	29	33	12.1	$p < 0.001$
NOX4 + fulvene-5	13	53	66	19.7	$p < 0.001$
NOX4 + 6-fulvene	10	30	40	25.0	$p = 0.0011$
NOX4 + proton sponge blue	9	30	39	23.1	$p < 0.001$
NOX4 + KN93	5	35	40	12.5	$p < 0.001$
NOX4 + AIP	3	41	44	6.8	$p < 0.001$

To quantitatively characterize the arrhythmic phenotype, the videos of beating hearts in real time were analyzed by taking sequential pictures generated from the videos using a custom-made line-scanning software LQ-1 (9, 10). Fig. 1*A* shows a representative *myl7*:*GFP* zebrafish embryo. The outline of the heart in Fig. 1*A* is marked with *green lines,* and the *white line* in Fig. 1*A* indicates the scanning line position of the LQ-1 program. Fig. 1*B* is a flow chart demonstrating video analyses and measurements of beat-to-beat intervals. *Red* and *yellow arrows* in Fig. 1*B* indicate relaxation and contraction of the heart, respectively. The *black arrow* in Fig. 1*B* indicates a beat-to-beat interval. Fig. 1*C* demonstrates heart beats from two representative embryos analyzed by the LQ-1 program. The heart beat of the control embryo was consistent and stable, whereas the NOX4-overexpressed embryos had irregular heart beats characterized by random early or late beats, as indicated by the *arrowheads* in Fig. 1*C*. Next, we measured the beat-to-beat intervals (time interval of two consecutive contractions) of each embryo. The beat-to-beat intervals of control embryos had small fluctuations as expected for normal physiology (23, 24). However, NOX4-overexpressed embryos had much more variable fluctuations in beat-to-beat interval. To quantitatively define the beat-to-beat fluctuation (beat-to-beat variation), we calculated the standard deviation of beat-to-beat intervals of each embryo, which has been previously employed as a quantitative assessment of cardiac arrhythmia (25, 26). As shown in Fig. 1*E*, the standard deviation of beat-to-beat intervals of a representative control embryo was 0.024 s/beat *versus* 0.035 s/beat for a representative NOX4 embryo. These are shown as the two *circled points* in Fig. 1*F*. The rest of the points in Fig. 1*F* are the standard deviations of individual embryos examined in the two groups ($p < 0.01$ control *versus* NOX4-injected). Of note, the LQ-1 analysis results represent the variations in beat-to-beat intervals for the representative videos of control, and NOX4 RNA-injected zebrafish embryos (supplemental Video I) are shown in Fig. 1*C*. The average heart rates of control and NOX4 embryos are indifferent (Fig. 1*D*) (93.3 ± 1.2 beats/min in control *versus* 96.4 ± 2.5 beats/min in NOX4-injected embryos).

NOX4-specific Morpholino Co-injection Prevented NOX4-induced Arrhythmia and Superoxide Production in Zebrafish—To examine a specific role for NOX4 in inducing arrhythmia in zebrafish, we co-injected NOX4 RNA with 3 ng of NOX4 morpholino, designed to target the translation initiation site of human NOX4 sequence. To compare with NOX4 RNA-injected embryos, we analyzed videos of co-injection embryos taken from three independent injections. Effects of different interventions on the arrhythmic phenotype of zebrafish embryos are summarized in Table 1. Interestingly, MO co-injection markedly reduced the percentage of embryos that developed arrhythmic phenotypes from 53 to 20%. Out of 251 embryos analyzed from the NOX4-injected group, 133 embryos developed arrhythmia characterized by frequent irregular beats and large beat-to-beat variation. However, among all the 59 NOX4 MO co-injected embryos analyzed, only 12 had phenotypes. These results suggest that the arrhythmic phenotype is specifically induced by NOX4 overexpression.

To further investigate the mechanisms underlying NOX4-induced arrhythmia, we measured superoxide production at 27–33 hpf when phenotypes appear. Previous studies have shown that the main product of NOX4 in the heart can either be superoxide or hydrogen peroxide (H_2O_2) (27, 28). Superoxide production in NOX4 RNA-injected zebrafish embryos, determined by ESR, was more than doubled to 10.9 μM/min/mg from 5.3 μM/min/mg in the controls (Fig. 2). Superoxide production in the MO co-injection group was significantly attenuated to control levels (Fig. 2). DCFH-DA is a cell-permeable H_2O_2 probe, commonly used as an indicator of the intracellular levels of H_2O_2 when it is permeabilized into the cells and de-esterified, and it becomes fluorescent upon oxidation by H_2O_2. This sensitive probe has been widely used in cells and also in zebrafish embryos (18, 29) to rapidly detect and quantify H_2O_2 production. Using DCFH-DA, we found that the H_2O_2 production was also significantly increased in NOX4-injected embryos (Fig. 3), which is consistent with our findings in atrial fibrillation patients (5).

Overexpression of NOX4 Mutant Deficient in NADPH Binding Had No Effect on Cardiac Phenotype—To test the hypothesis that NOX4 induces arrhythmia by increasing NADPH-driven ROS production in zebrafish embryos, we generated full-length mutant RNA of NOX4-P437H, in which the proline to histidine mutation inactivates the superoxide generating activity of NOX4 by disrupting NADPH binding (27). We injected the same amount of RNA of NOX4-P437H (300 pg) into the embryos and then analyzed the videos of control and NOX4-P437H embryos with LQ-1 (Fig. 4*B*). Similarly, we also compared the beat-to-beat interval of each embryo in control and the NOX4-P437H group. All the embryos from both groups shared the same range of beat-to-beat variation (Fig. 4*A*).

Next, we measured superoxide levels in these two groups. Overexpression of NOX4-P437H failed to increase superoxide

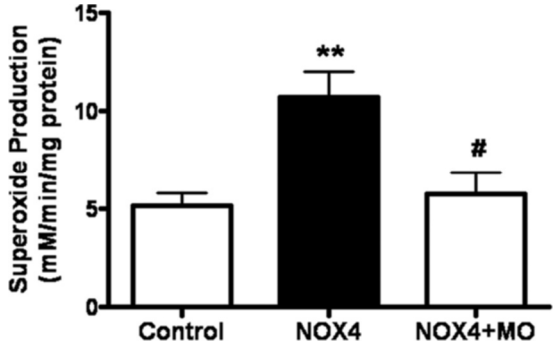

FIGURE 2. **NOX4 overexpression results in increased superoxide in zebrafish embryos that is attenuated by NOX4 morpholino co-injection.** Superoxide production from control and NOX4 RNA-injected zebrafish embryos was determined by electron spin resonance. *MO*, NOX4 morpholino. **, $p < 0.01$ *versus* control group; #, $p < 0.05$ *versus* NOX4 group. $n = 12$, 10, and 3, respectively.

production (Fig. 4*C*). This is consistent with a previous observation that overexpression of NOX4-P437H transgene in the heart abolishes superoxide generation activity from NOX4 (27). Therefore, the NADPH-driven superoxide generating activity of NOX4 indeed seems to be required for NOX4 overexpression-induced arrhythmia in zebrafish.

Role of NOX4-derived ROS in Mediating Cardiac Arrhythmia in Zebrafish—To further examine an intermediate role of ROS in NOX4-dependent arrhythmogenesis, we treated NOX4-injected embryos with a pharmacological ROS scavenger and different NOX/NOX4 inhibitors. Titrations of chemicals were carried out with un-injected embryos first to find the optimal concentrations of these drugs, which did not cause any morphological deficiencies when used alone. Pretreatment with PEG-SOD (25 units/ml) or Tempo (10 μM) before 24 hpf, when the heart starts contracting, was able to prevent NOX4-induced ROS production and development of the arrhythmic phenotype (Figs. 3 and 5*A* and Table 1). Fulvene-5 inhibits NOX4 activity to 40% at 5 μM in cells (30). In our treatments, we found that fulvene-5 at 10 μM starting before 24 hpf significantly abolished NOX4-induced ROS production and arrhythmic phenotype (Figs. 3 and 5*B* and Table 1). Similar effects were also observed in 6-dimethylamino-fulvene, another fulvene derivative, and proton sponge blue-treated NOX4 embryos (Fig. 5*C* and Table 1). Proton sponge blue has been previously shown to inactivate NOX4 in cell culture (31, 32). These data strongly suggest that NOX4 overexpression-induced arrhythmogenesis is dependent on NOX4 activity and ROS production in zebrafish.

Role of ROS-activated CaMKII in Mediating NOX4 Overexpression-induced Cardiac Arrhythmia—CaMKII is a potential pro-arrhythmic enzyme. Substrates of CaMKII include ion channels known to regulate intracellular calcium/sodium/potassium handling to impact cell physiology. Phosphorylation at Thr-286/287 results in persistent CaMKII activity (33). Therefore, we next examined whether activation of CaMKII mediates NOX4-induced arrhythmogenesis. Interestingly, at 24 hpf, the time point right before we observed arrhythmic phenotype and also when the zebrafish heart starts beating, CaMKII Thr-286 phosphorylation was significantly increased in NOX4-injected embryos (Fig. 6*A*). This can be followed up to 31 hpf (1.38-fold) (Fig. 6*B*), although it was less potent than at 24 hpf (1.65-fold).

Phosphorylation of CaMKII was also inhibited by PEG-SOD treatment as demonstrated by Western blotting (Fig. 6*C*) and whole mount immunohistochemistry (Fig. 7*D*, for detailed experimental procedures see under "Experimental Procedures" and Fig. 7 legend), implicating redox-sensitive activation of CaMKII. Treatment of embryos with autocamtide-2 related inhibitory peptide II (AIP), a selective CaMKII inhibitor, or KN93 completely abolished the arrhythmic phenotype induced by NOX4 RNA injection (Table 1). In Table 1, the total number of embryos analyzed and the number of embryos that developed the arrhythmic phenotype or not are presented in detail for each interventional protocol. Taken together, these data demonstrate a NOX4/ROS/CaMKII pathway in inducing cardiac arrhythmia in zebrafish.

DISCUSSION

The most significant finding of this study is the first identification of a causal role of NOX4 in the development of cardiac arrhythmia. Injection of wild type human NOX4 RNA, but not an enzyme-inactive mutant RNA or co-injection with MO, resulted in reproducible cardiac arrhythmic phenotype in zebrafish embryos. The arrhythmia is characterized by irregular heartbeats that are defined by a highly variable beat-to-beat interval, quantitatively analyzed using a custom-made but previously established LQ-1 program (9, 10). The phenotype was also preventable by scavenging superoxide with PEG-SOD/Tempo or inhibiting NOX4 with fulvene-5, 6-dimethylamino-fulvene, or proton sponge blue. Inhibition of CaMKII activation with AIP was effective in attenuating NOX4 overexpression-induced arrhythmic phenotype. These data clearly establish that NOX4 activation could lead to NADPH binding-dependent ROS production and subsequent CaMKII activation and arrhythmogenesis.

The NADPH oxidase family is evolutionarily conserved and plays a major role in ROS production across many different organisms. Members of the NOX family have been identified in various organisms, including mammal, avian, amphibian, fish, and plants (34). By using zebrafish as an *in vivo* model, we studied the possible link between NOX-produced ROS and cardiac disorders. We also examined the potential interaction between overexpressed human NOX4 and endogenous zebrafish NOX family members to exclude nonspecific phenotypes caused by regulation of other NOX isoforms. The full sequence of the zebrafish NOX4 has not yet been reported, except for three fragments on Ensemble predicted by alignment. By alignment and RT-PCR, we amplified part of zebrafish NOX4 from zebrafish cDNA (data not shown), which showed high similarity and shared the same functional domains as the mammalian homolog (35). Similar analyses were performed for identifying zebrafish NOX1/2. Effects of human NOX4 RNA injection on zebrafish NOX1/2/4 mRNA expression through different developmental stages of zebrafish embryos were determined by RT-PCR analyses (Fig. 7). Zebrafish NOX1 levels increased at 24 hpf but dropped at 48 hpf. Zebrafish NOX2 was hardly detectable at early stages (6 hpf) but increased and stayed up through 24 to 48 hpf. Zebrafish NOX4 expression was similar

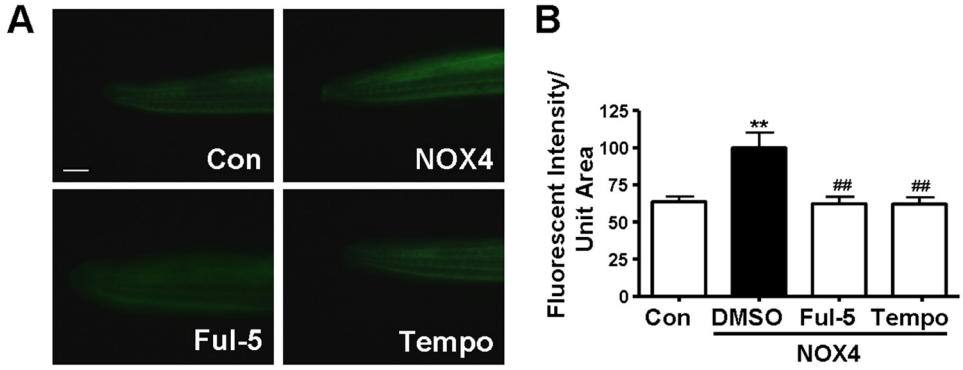

FIGURE 3. **NOX4 overexpression increases superoxide-dependent H_2O_2 production in zebrafish embryos.** *A,* images of DCFH-DA staining indicating endogenous H_2O_2 generation in tails of zebrafish embryos. The *scale bar* indicates 100 μm. *B,* arbitrary units of mean density of DCFH-DA signals quantified by ImageJ. *Ful-5,* fulvene-5, 10 μM; Tempo, 10 μM. **, $p < 0.01$ *versus* control (*Con*); ##, $p < 0.01$ *versus* NOX4/DMSO group. $n = 21$, 13, 15, and 20 from three injections.

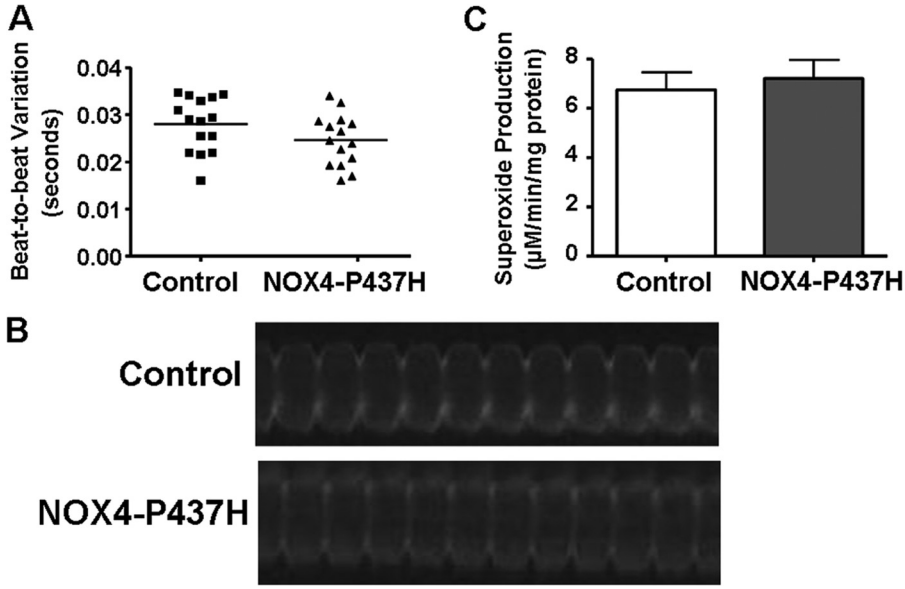

FIGURE 4. **Overexpression of NOX4 mutant deficient in NADPH binding had no effect on cardiac phenotype.** *A,* distributions of beat-to-beat variations of control and NOX4-P437H RNA-injected zebrafish embryos at 24–30 hpf. $n = 15$. *B,* representative LQ-1 results and analyses of beat-to-beat intervals in control and NOX4-P437H embryos. *C,* superoxide production in control and NOX4-P437H embryos. $n = 5$.

between 6 and 48 hpf. Overall, no change on endogenous NOX1/2/4 expression was observed upon hNOX4 overexpression, at least at an mRNA level, excluding the possibility of off-target effects of induction of other NOX isoforms. The hNOX4 signal reflected successful induction of the gene and decay of RNA after 48 h. Interestingly, zebrafish NOX1 and NOX4 might play a role in early development, based on their mRNA expression profiles from our 6 hpf data. Embryos of 6 hpf already produced a certain level of superoxide as measured by ESR (data not shown), indicating that ROS is possibly involved in an early stage of embryonic development.

Oxidative stress has been implicated in the development of AF, although a causal relationship has not been defined (4). In this study, we found that NADPH-driven ROS production from NOX4 induces arrhythmic phenotypes. In endothelium-specific NOX4 transgenic mice, the hydrogen peroxide level was increased in primary cultured endothelial cells and the aorta (36, 37). In the cardiac-specific NOX4 knock-out or transgenic mice, basal superoxide production was significantly decreased in the NOX4 knock-out mice, and it increased in transgenic mice (27, 28). In our zebrafish model, both superoxide and H_2O_2 levels were increased by NOX4 overexpression. Tempo treatment prevented the increase in H_2O_2 production in NOX4-injected embryos (Fig. 3), implicating that H_2O_2 is likely coming from NOX4-derived superoxide, rather than being generated directly by NOX4. We have also confirmed interaction between human NOX4 and zebrafish p22phox in 293 cells, by co-transfecting Myc-tagged NOX4 with HA-tagged p22phox, and immunoblotting for p22phox using an HA antibody after immunoprecipitation with a Myc antibody (supplemental Fig. III).

To investigate the specificity of NOX4 in inducing arrhythmia, the enzyme-inactive NOX4 mutant (NOX4-P437H) RNA was used. The proline to histidine mutation was first found in X-linked chronic granulomatous disease and tested to inactivate NOX2 (38), NOX3 (39), and NOX4 (27) superoxide generating activity, without changing the integrity of the protein. By examining the phenotype of NOX4-P437H embryos, we found that mutant NOX4 RNA cannot induce superoxide production or arrhythmogenesis. Similar to our observations,

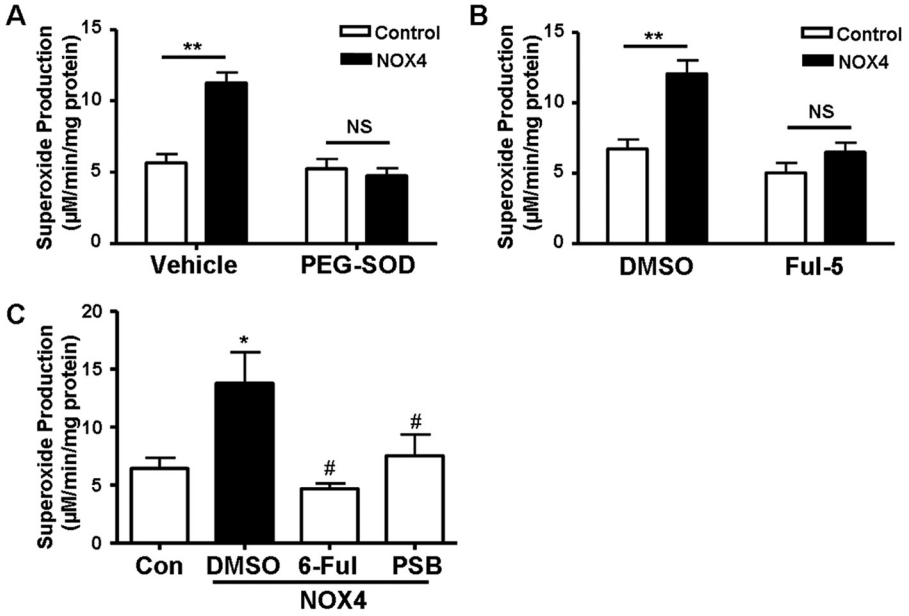

FIGURE 5. **Superoxide dismutase or NOX/NOX4 inhibitors attenuate superoxide production in NOX4-overexpressed zebrafish embryos.** Superoxide production in PEG-SOD (25 units/ml) (*A*), fulvene-5 (*Ful-5*, 10 μM) (*B*), 6-dimethylamino-fulvene (*6-Ful*, 10 μM), or proton sponge blue (*PSB*, 5 μM) (*C*)-treated zebrafish embryos started at 22–23 hpf. **, $p < 0.01$ *versus* control; *NS,* not significant *versus* control. *, $p < 0.05$ *versus* control; #, $p < 0.05$ *versus* NOX4 group. $n = 4$ for PEG-SOD, $n = 4$ for Ful-5, and $n = 3$ for 6-dimethylamino-fulvene and proton sponge blue treatments, respectively.

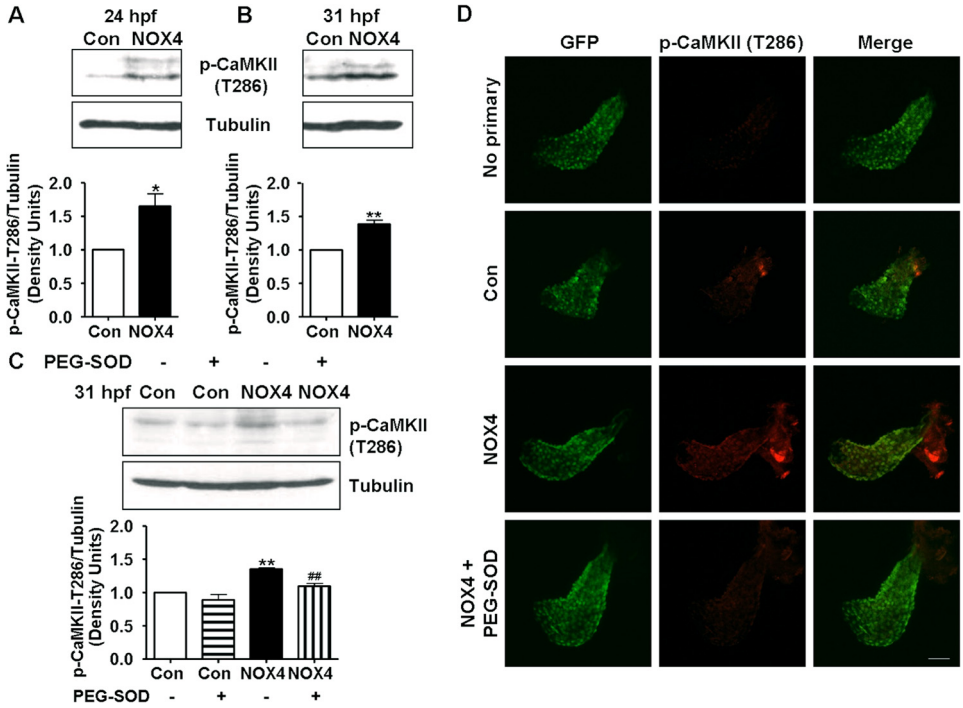

FIGURE 6. **NOX4 overexpression activates CaMKII in a superoxide-dependent fashion in zebrafish embryos.** Representative Western blot and quantitative data of CaMKII phosphorylation (Thr-286) at 24 hpf (*A*) and 31 hpf (*B*). $n = 4$. *, $p < 0.05$; **, $p < 0.01$ *versus* control group. *C,* representative Western blot and quantitative data of CaMKII phosphorylation (Thr-286) in PEG-SOD-treated embryos at 31 hpf. $n = 3$. **, $p < 0.01$ *versus* control; ##, $p < 0.01$ *versus* NOX4 group. *D,* confocal Z-stack images of heart (31–32 hpf) from indicated embryos. The *scale bar* is set at 50 μm. *No primary*, no primary antibody incubation as negative control.

superoxide production was found inhibited in NOX4-P437H transgenic mice, as measured by dihydroethidium fluorescent intensity (27). Besides genetic approaches of MO co-injection and NOX4-P437H mutant RNA injection, we also tested the effects of NOX4 inhibitors fulvene-5, 6-dimethylamino-fulvene, and proton sponge blue. All of these agents effectively attenuated arrhythmic phenotypes and superoxide production induced by NOX4 RNA injection.

Activation of CaMKII has been linked to arrhythmia, hypertrophy, and apoptosis in the heart. Phosphorylation at Thr-286 in the autoinhibitory domain of CaMKII prevents re-association of the kinase domain to result in persistent CaMKII acti-

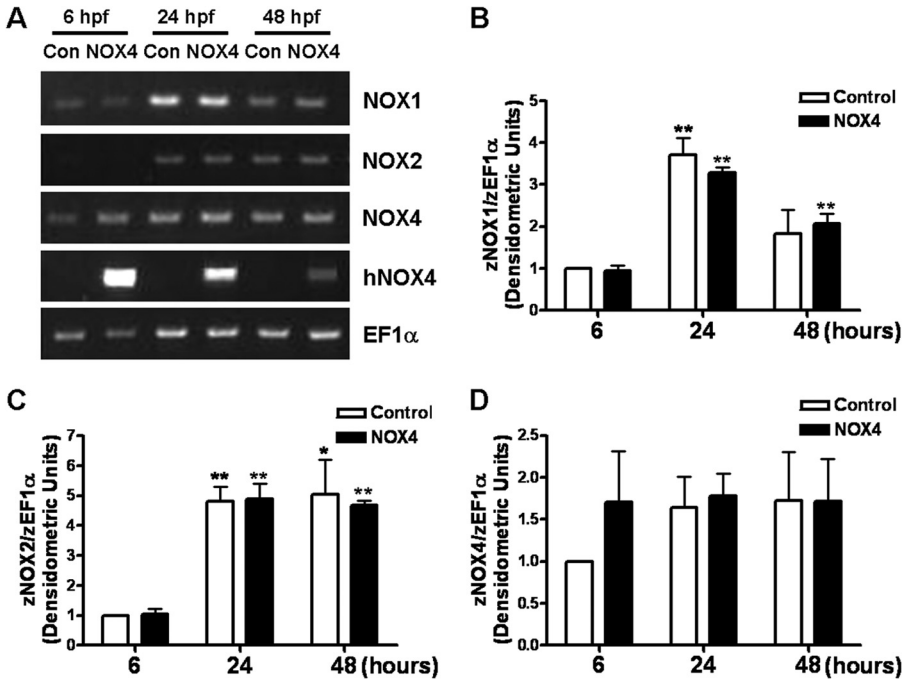

FIGURE 7. **Levels of endogenous zebrafish NOX1, NOX2, and NOX4 isoforms were not affected by injection of human NOX4 RNA.** *A,* representative RT-PCR results of zebrafish NOX1/2/4 and human NOX4 expression through different developmental stages. Same amount of cDNA was used as template in each PCR. *B–D,* quantitative analyses of zebrafish NOX1/2/4 at indicated times from RT-PCR results. The housekeeping gene *ef1α* was used as an internal control. Gene expression level was normalized to the control group at 6 hpf. *, $p < 0.05$; **, $p < 0.01$ compared with 6 hpf. No difference was found between control and NOX4 groups. $n = 3$. Note that interestingly, although zebrafish NOX4 was expressed at an earlier stage of the development (6 hpf), the zebrafish NOX1/2 isoforms only became detectable after 24 hpf.

vation. Another possibility to activate CaMKII is direct oxidation of paired Met residues at Met-281/Met-282 sites by ROS (40), which is not regulated by NOX4 overexpression (supplemental Fig. IV). Seven CaMKII genes have been identified in zebrafish so far (41, 42). *In situ* hybridization indicates that CaMKII can be detected since the commencement of zygotic expression (42). In our study, we examined CaMKII Thr-286 phosphorylation by immunoblot and immunohistochemistry, and we observed a significant increase of CaMKII Thr-286 phosphorylation in NOX4-overexpressed embryos. The CaMKII activation was attenuated by PEG-SOD, implicating that it is downstream of the NOX4/ROS axis. A selective inhibitor for CaMKII, AIP, or KN93 abrogated the arrhythmic phenotype in response to NOX4 RNA injection. Therefore, phosphorylation-dependent activation of CaMKII at least partially underlies NOX4-dependent arrhythmogenesis.

In summary, our data for the first time elucidate a novel mechanism underlying development of cardiac arrhythmia, namely NOX4 activation, consequent NADPH-driven ROS production, and redox-sensitive activation of CaMKII. These findings may ultimately lead to novel therapeutics targeting NOX4 for the treatment or prevention of cardiac arrhythmia.

REFERENCES

1. Cai, H., Li, Z., Goette, A., Mera, F., Honeycutt, C., Feterik, K., Wilcox, J. N., Dudley, S. C., Jr., Harrison, D. G., and Langberg, J. J. (2002) Downregulation of endocardial nitric oxide synthase expression and nitric oxide production in atrial fibrillation: potential mechanisms for atrial thrombosis and stroke. *Circulation* **106,** 2854–2858
2. Kim, Y. M., Guzik, T. J., Zhang, Y. H., Zhang, M. H., Kattach, H., Ratnatunga, C., Pillai, R., Channon, K. M., and Casadei, B. (2005) A myocardial Nox2 containing NAD(P)H oxidase contributes to oxidative stress in human atrial fibrillation. *Circ. Res.* **97,** 629–636
3. Dudley, S. C., Jr., Hoch, N. E., McCann, L. A., Honeycutt, C., Diamandopoulos, L., Fukai, T., Harrison, D. G., Dikalov, S. I., and Langberg, J. (2005) Atrial fibrillation increases production of superoxide by the left atrium and left atrial appendage: role of the NADPH and xanthine oxidases. *Circulation* **112,** 1266–1273
4. Youn, J. Y., Zhang, J., Zhang, Y., Chen, H., Liu, D., Ping, P., Weiss, J. N., and Cai, H. (2013) Oxidative stress in atrial fibrillation: an emerging role of NADPH oxidase. *J. Mol. Cell. Cardiol.* **62,** 72–79
5. Zhang, J., Youn, J. Y., Kim, A. Y., Ramirez, R. J., Gao, L., Ngo, D., Chen, P., Scovotti, J., Mahajan, A., and Cai, H. (2012) NOX4-dependent hydrogen peroxide overproduction in human atrial fibrillation and HL-1 atrial cells: relationship to hypertension. *Front Physiol.* **3,** 140
6. Bakkers, J. (2011) Zebrafish as a model to study cardiac development and human cardiac disease. *Cardiovasc. Res.* **91,** 279–288
7. Chen, J. N., Haffter, P., Odenthal, J., Vogelsang, E., Brand, M., van Eeden, F. J., Furutani-Seiki, M., Granato, M., Hammerschmidt, M., Heisenberg, C. P., Jiang, Y. J., Kane, D. A., Kelsh, R. N., Mullins, M. C., and Nüsslein-Volhard, C. (1996) Mutations affecting the cardiovascular system and other internal organs in zebrafish. *Development* **123,** 293–302
8. Langenbacher, A. D., Dong, Y., Shu, X., Choi, J., Nicoll, D. A., Goldhaber, J. I., Philipson, K. D., and Chen, J. N. (2005) Mutation in sodium-calcium exchanger 1 (NCX1) causes cardiac fibrillation in zebrafish. *Proc. Natl. Acad. Sci. U.S.A.* **102,** 17699–17704
9. Nguyen, C. T., Lu, Q., Wang, Y., and Chen, J. N. (2008) Zebrafish as a model for cardiovascular development and disease. *Drug Discov. Today Dis. Models* **5,** 135–140
10. Lu, G., Ren, S., Korge, P., Choi, J., Dong, Y., Weiss, J., Koehler, C., Chen, J. N., and Wang, Y. (2007) A novel mitochondrial matrix serine/threonine protein phosphatase regulates the mitochondria permeability transition pore and is essential for cellular survival and development. *Genes Dev.* **21,** 784–796
11. Burns, C. G., Milan, D. J., Grande, E. J., Rottbauer, W., MacRae, C. A., and Fishman, M. C. (2005) High-throughput assay for small molecules that modulate zebrafish embryonic heart rate. *Nat. Chem. Biol.* **1,** 263–264

12. Oak, J. H., and Cai, H. (2007) Attenuation of angiotensin II signaling recouples eNOS and inhibits nonendothelial NOX activity in diabetic mice. *Diabetes* **56,** 118–126
13. Chalupsky, K., and Cai, H. (2005) Endothelial dihydrofolate reductase: critical for nitric oxide bioavailability and role in angiotensin II uncoupling of endothelial nitric oxide synthase. *Proc. Natl. Acad. Sci. U.S.A.* **102,** 9056–9061
14. Gao, L., Chalupsky, K., Stefani, E., and Cai, H. (2009) Mechanistic insights into folic acid-dependent vascular protection: dihydrofolate reductase (DHFR)-mediated reduction in oxidant stress in endothelial cells and angiotensin II-infused mice: a novel HPLC-based fluorescent assay for DHFR activity. *J. Mol. Cell. Cardiol.* **47,** 752–760
15. Zhang, J., and Cai, H. (2010) Netrin-1 prevents ischemia/reperfusion-induced myocardial infarction via a DCC/ERK1/2/eNOS s1177/NO/DCC feed-forward mechanism. *J. Mol. Cell. Cardiol.* **48,** 1060–1070
16. Youn, J. Y., Gao, L., and Cai, H. (2012) The p47phox- and NADPH oxidase organiser 1 (NOXO1)-dependent activation of NADPH oxidase 1 (NOX1) mediates endothelial nitric oxide synthase (eNOS) uncoupling and endothelial dysfunction in a streptozotocin-induced murine model of diabetes. *Diabetologia* **55,** 2069–2079
17. Li, J., Umar, S., Iorga, A., Youn, J. Y., Wang, Y., Regitz-Zagrosek, V., Cai, H., and Eghbali, M. (2012) Cardiac vulnerability to ischemia/reperfusion injury drastically increases in late pregnancy. *Basic Res. Cardiol.* **107,** 271
18. Kishi, S., Bayliss, P. E., Uchiyama, J., Koshimizu, E., Qi, J., Nanjappa, P., Imamura, S., Islam, A., Neuberg, D., Amsterdam, A., and Roberts, T. M. (2008) The identification of zebrafish mutants showing alterations in senescence-associated biomarkers. *PLoS Genet.* **4,** e1000152
19. Chen, J. N., and Fishman, M. C. (1996) Zebrafish tinman homolog demarcates the heart field and initiates myocardial differentiation. *Development* **122,** 3809–3816
20. Elahi, M. M., Flatman, S., and Matata, B. M. (2008) Tracing the origins of postoperative atrial fibrillation: the concept of oxidative stress-mediated myocardial injury phenomenon. *Eur. J. Cardiovasc. Prev. Rehabil.* **15,** 735–741
21. Kim, Y. M., Kattach, H., Ratnatunga, C., Pillai, R., Channon, K. M., and Casadei, B. (2008) Association of atrial nicotinamide adenine dinucleotide phosphate oxidase activity with the development of atrial fibrillation after cardiac surgery. *J. Am. Coll. Cardiol.* **51,** 68–74
22. Chang, J. P., Chen, M. C., Liu, W. H., Yang, C. H., Chen, C. J., Chen, Y. L., Pan, K. L., Tsai, T. H., and Chang, H. W. (2011) Atrial myocardial nox2 containing NADPH oxidase activity contribution to oxidative stress in mitral regurgitation: potential mechanism for atrial remodeling. *Cardiovasc. Pathol.* **20,** 99–106
23. Chan, P. K., Lin, C. C., and Cheng, S. H. (2009) Noninvasive technique for measurement of heartbeat regularity in zebrafish (*Danio rerio*) embryos. *BMC Biotechnol.* **9,** 11
24. Schwerte, T., Prem, C., Mairösl, A., and Pelster, B. (2006) Development of the sympatho-vagal balance in the cardiovascular system in zebrafish (*Danio rerio*) characterized by power spectrum and classical signal analysis. *J. Exp. Biol.* **209,** 1093–1100
25. Incardona, J. P., Carls, M. G., Day, H. L., Sloan, C. A., Bolton, J. L., Collier, T. K., and Scholz, N. L. (2009) Cardiac arrhythmia is the primary response of embryonic Pacific herring (*Clupea pallasi*) exposed to crude oil during weathering. *Environ. Sci. Technol.* **43,** 201–207
26. Zhang, Y., Huang, L., Zuo, Z., Chen, Y., and Wang, C. (2013) Phenanthrene exposure causes cardiac arrhythmia in embryonic zebrafish via perturbing calcium handling. *Aquat. Toxicol.* **142,** 26–32
27. Ago, T., Kuroda, J., Pain, J., Fu, C., Li, H., and Sadoshima, J. (2010) Upregulation of Nox4 by hypertrophic stimuli promotes apoptosis and mitochondrial dysfunction in cardiac myocytes. *Circ. Res.* **106,** 1253–1264
28. Kuroda, J., Ago, T., Matsushima, S., Zhai, P., Schneider, M. D., and Sadoshima, J. (2010) NADPH oxidase 4 (Nox4) is a major source of oxidative stress in the failing heart. *Proc. Natl. Acad. Sci. U.S.A.* **107,** 15565–15570
29. Kang, K. A., Zhang, R., Lee, K. H., Chae, S., Kim, B. J., Kwak, Y. S., Park, J. W., Lee, N. H., and Hyun, J. W. (2006) Protective effect of triphlorethol-A from *Ecklonia cava* against ionizing radiation *in vitro*. *J. Radiat. Res.* **47,** 61–68
30. Bhandarkar, S. S., Jaconi, M., Fried, L. E., Bonner, M. Y., Lefkove, B., Govindarajan, B., Perry, B. N., Parhar, R., Mackelfresh, J., Sohn, A., Stouffs, M., Knaus, U., Yancopoulos, G., Reiss, Y., Benest, A. V., Augustin, H. G., and Arbiser, J. L. (2009) Fulvene-5 potently inhibits NADPH oxidase 4 and blocks the growth of endothelial tumors in mice. *J. Clin. Invest.* **119,** 2359–2365
31. Munson, J. M., Fried, L., Rowson, S. A., Bonner, M. Y., Karumbaiah, L., Diaz, B., Courtneidge, S. A., Knaus, U. G., Brat, D. J., Arbiser, J. L., and Bellamkonda, R. V. (2012) Anti-invasive adjuvant therapy with imipramine blue enhances chemotherapeutic efficacy against glioma. *Sci. Transl. Med.* 10.1126/scitranslmed.3003016
32. Perry, B. N., Govindarajan, B., Bhandarkar, S. S., Knaus, U. G., Valo, M., Sturk, C., Carrillo, C. O., Sohn, A., Cerimele, F., Dumont, D., Losken, A., Williams, J., Brown, L. F., Tan, X., Ioffe, E., Yancopoulos, G. D., and Arbiser, J. L. (2006) Pharmacologic blockade of angiopoietin-2 is efficacious against model hemangiomas in mice. *J. Invest. Dermatol.* **126,** 2316–2322
33. Hudmon, A., and Schulman, H. (2002) Structure-function of the multifunctional Ca^{2+}/calmodulin-dependent protein kinase II. *Biochem. J.* **364,** 593–611
34. Kawahara, T., Quinn, M. T., and Lambeth, J. D. (2007) Molecular evolution of the reactive oxygen-generating NADPH oxidase (Nox/Duox) family of enzymes. *BMC Evol. Biol.* **7,** 109
35. Corpet, F. (1988) Multiple sequence alignment with hierarchical clustering. *Nucleic Acids Res.* **16,** 10881–10890
36. Craige, S. M., Chen, K., Pei, Y., Li, C., Huang, X., Chen, C., Shibata, R., Sato, K., Walsh, K., and Keaney, J. F., Jr. (2011) NADPH oxidase 4 promotes endothelial angiogenesis through endothelial nitric oxide synthase activation. *Circulation* **124,** 731–740
37. Ray, R., Murdoch, C. E., Wang, M., Santos, C. X., Zhang, M., Alom-Ruiz, S., Anilkumar, N., Ouattara, A., Cave, A. C., Walker, S. J., Grieve, D. J., Charles, R. L., Eaton, P., Brewer, A. C., and Shah, A. M. (2011) Endothelial Nox4 NADPH oxidase enhances vasodilatation and reduces blood pressure *in vivo*. *Arterioscler. Thromb. Vasc. Biol.* **31,** 1368–1376
38. Dinauer, M. C., Curnutte, J. T., Rosen, H., and Orkin, S. H. (1989) A missense mutation in the neutrophil cytochrome *b* heavy chain in cytochrome-positive X-linked chronic granulomatous disease. *J. Clin. Invest.* **84,** 2012–2016
39. Ueno, N., Takeya, R., Miyano, K., Kikuchi, H., and Sumimoto, H. (2005) The NADPH oxidase Nox3 constitutively produces superoxide in a p22phox-dependent manner: its regulation by oxidase organizers and activators. *J. Biol. Chem.* **280,** 23328–23339
40. Erickson, J. R., Joiner, M. L., Guan, X., Kutschke, W., Yang, J., Oddis, C. V., Bartlett, R. K., Lowe, J. S., O'Donnell, S. E., Aykin-Burns, N., Zimmerman, M. C., Zimmerman, K., Ham, A. J., Weiss, R. M., Spitz, D. R., Shea, M. A., Colbran, R. J., Mohler, P. J., and Anderson, M. E. (2008) A dynamic pathway for calcium-independent activation of CaMKII by methionine oxidation. *Cell* **133,** 462–474
41. Rothschild, S. C., Easley, C. A., 4th, Francescatto, L., Lister, J. A., Garrity, D. M., and Tombes, R. M. (2009) Tbx5-mediated expression of Ca^{2+}/calmodulin-dependent protein kinase II is necessary for zebrafish cardiac and pectoral fin morphogenesis. *Dev. Biol.* **330,** 175–184
42. Rothschild, S. C., Lister, J. A., and Tombes, R. M. (2007) Differential expression of CaMK-II genes during early zebrafish embryogenesis. *Dev. Dyn.* **236,** 295–305